Proceedings of Ninth World Conference on Earthquake Engineering
August 2-9, 1988, Tokyo-Kyoto, JAPAN (Vol.IV)

6-4-21

EARTHQUAKE DAMAGE INDEX FOR REINFORCED CONCRETE COLUMNS

Junji OGAWA[1] and Toshio SHIGA[2]

1 Earthquake Engineering Research Institute, Faculty of Engineering,
Tohoku University, Sendai, Japan

2 Department of Civil Engineering, Faculty of Engineering,
Tohoku Gakuin University, Sendai, Japan

SUMMARY

The cantilever-type full scale reinforced concrete test specimens representing the first story interior columns in medium-rise buildings in Japan were tested up to failure under static cyclic unidirectional reversal loading. Concrete crack patterns and concrete spalling area were measured at several displacement ductilities during loading. The equivalent crack area ratio and the equivalent spalling area ratio were calculated, and proposed as damage indices of reinforced concrete structures. If crack height is more than one column depth, the displacement ductility should be more than 1. If concrete spalling exists, the displacement ductility should be more than 5.

INTRODUCTION

In current earthquake-resistant design of reinforced concrete buildings, it is necessary to permit some degree of damage to the structural elements, when subjected to severe earthquake excitations. Some indicators for evaluating structural damage of reinforced concrete buildings are proposed, such as damage ratio (1), flexural damage ratio and dissipated energy (2), slope ratio (3), energy dissipation index (4), etc. However, the application of these indicators for damaged buildings after the earthquake are not practical, because those indicators need hysteresis loops during the earthquake. But no building has measuring equipments to record the load displacement time-histories. The visual inspection of the damaged buildings is the only way to evaluate the structural damage states. Main data from the visual inspection are the information on concrete cracks and concrete spalling. In this paper, the relation between the displacement ductility and the information on cracks and spalling area is examined on the basis of test results.

TEST SPECIMEN, LOADING SYSTEM AND TESTING PROCEDURE

In order to simplify the response characteristics of the test specimen, the cantilever type columns were used in this experimental program. The specimens are approximately full scale models, considered representative of the first story interior columns in medium-rise buildings in Japan. The test specimen had the configuration shown in Fig. 1. Each column was a 1,400 mm long cantilever, having gross cross section of 500 mm by 500 mm, cast in a vertical position. The lateral load was applied at a distance of 1,100 mm from the intersection between the column and the footing block. So, the shear span ratio (H/D) was 2.2.

The footing block of a test specimen and the reaction steel frames were prestressed to an extremely rigid testing floor (thickness = 900 mm) with high strength steel rods. The lateral loading system was made up of two hydraulic oil jacks (capacity compression 50t). One was for the positive direction loading (to the North) and the other for the negative direction loading (to the South). The axial load was applied to the column free end. The axial loading system was made up of a loading beam, a pair of high strength steel rods and two hydraulic center hole jacks (capacity compression 100t). For the sake of safety and stability of the axial loading system, the loading beam was built in C-shape, to make the connecting surfaces with pulling rods lower than the column free end surface, like a balancing toy. The hydraulic pressure for those jacks was provided by two portable hydraulic pumps (capacity 0.5 l/min., 720 kg/cm^2). The pump for the axial loading jacks was controlled automatically. The pump for the lateral loading jacks was controlled manually, with applied loads varied to follow approximately the prescribed displacement for force histories. The target displacement histories are shown in Fig. 2. The first yield displacement of 5.5 mm (1/200 radians) for LC-1 was determined from the average value of 5.86 mm and -4.99 mm, at which one of the longitudinal tension reinforcement strain exceeded yield strain of $2100*10^{-6}$. The other specimens yielded around this value.

The axial load values fell into two groups. One was 13 % of the ultimate axial load, applied to LC-1 through LC-4 (axial load = 75t). The other was 25 % of that, applied to LC-5 (130t), and LC10 through LC12 (155t). The ultimate axial load was obtained with multiplying the 28-day compressive strength of the concrete by the gross sectional area of the column. All specimens were coated with white emulsion paint to make cracks in the concrete more visible. Whenever cracks were found during the loading, cracks were marked black with a pencil, so that the crack patterns could be followed easily. At every time of the loading stage at which the residual displacement became zero, crack patterns and outlines of concrete spalling were traced with a fiber tip pen on a transparent thin plastics sheet. The width of the plastics sheet was just the same as the column width, in order to make it easy to set the sheet on the very same position at each tracing of crack patterns and outlines of spalling. The cracks at the intersection between the column and the footing block were not traced.

INSTRUMENTATION

Instrumentation measured lateral and vertical column displacements, column loads, axial load, deformations of the column along one of the column surfaces, and strain of longitudinal and transverse reinforcement. Displacements of the column, relative to a stiff reference frame attached to the footing block, were measured at the loading point using LVDTs. The LVDTs at the loading point were mounted to the column with specially fabricated revolving jigs. Other LVDTs were mounted to the reference frame at heights of 100, 300, 500, 700, and 900 mm from the footing block surface. Any movement of the footing block during testing does not influence the recorded displacements. Strain-gauged load cells were mounted to the hydraulic jacks for axial and lateral loads. Electrical resistance strain gauges having 2 mm gauge length were bonded on longitudinal and transverse reinforcement at various points in the specimen. All signals were scanned at discrete intervals using a low-speed scanner box. The signals were stored digitally on a computer floppy disk. Signals of displacement and load were monitored in analog form on a X-Y recorder.

TEST RESULTS

Load-displacement hysteresis loops of LC12 are shown in Fig. 3. These loops are very stable up to displacement ductility (D.D.) of 10. The test specimen reached the ultimate load (41.1t) at D.D. of 3. Lateral loads reported in this figure were made corrections for the lateral component of the force in the axial

load jacks. Twist of the column about the column longitudinal axis could be determined from LVDTs readings, and was observed to be negligible.

Concrete cracks and concrete spalling area diagrams of LC12 are shown in Fig. 4. As the load increased, the amount of cracks increased. Primary cracks were generally horizontal, and were apparently due to flexural effects. Diagonal cracks formed on the nonloading surfaces parallel to the lateral load direction. Horizontal cracks formed on the loading surfaces. After D.D. of 2, development of new cracks slowed, but when larger D.D. applied, crack width of some major existing cracks became larger. The specimens did not begin concrete spalling until D.D. of 5. As the D.D. increased more than 5, concrete spalling increased.

Cracks and outlines of the concrete spalling area were manually divided into small multi-linear segments at an adequate length by manual operation. Vector data of each segment were obtained with a tablet digitizer. After setting a computer display as 500 pixels representing the column width of 500 mm, crack patterns were drawn with blue lines on the display, using vector data of cracks. If concrete spalling area data exist, outlines of the spalling area should be drawn with red lines on the same display, and painted the inside of these figures with red, in order to delete cracks, included in the spalling area. The equivalent crack area was obtained by counting up the number of blue pixels on the display. Equivalent concrete crack area ratios and equivalent concrete spalling area ratios could be calculated with this method.

Relations for all test specimens between equivalent crack area ratio and displacement ductility are shown in Fig. 5. Equivalent crack area ratios in these figures are calculated from limited area data, included in the core concrete surface within one column depth height from the footing block. As the D.D. increases up to 5, crack ratios increase. After reaching D.D. of 5, crack ratios decrease rapidly due to the effect of concrete spalling. Crack ratios of the 13 % axial load group are slightly larger than that of the 25 % group.

Relations for all test specimens between equivalent spalling area ratio and displacement ductility are shown in Fig. 6. The very same calculation method as Fig. 5 is followed. Specimens do not begin concrete spalling until D.D. of 5. As the D.D. increases more than 5, spalling ratio increases. Spalling ratios of the 25 % axial load group are larger than that of the 13 %. Spalling ratios of the loading surfaces are much larger than that of the nonloading surface.

CONCLUSIONS

Based on the results of this experimental program, in which the cantilever type full scale model specimens of reinforced concrete columns were subjected to static unidirectional reversal loading, the following conclusions were deduced:

1) The cracking starts around D.D. of 0.5. As the D.D. increases, the equivalent crack area ratio increases rapidly. If the D.D. is less than 1, the highest height of cracks should be less than one column depth. During D.D. range from 2 to 5, development of new cracks slows, and crack width of some existing cracks becomes wider. After reaching D.D. of 5 to 7, the concrete spalling starts. Thereafter, the equivalent spalling ratio increases rapidly, then the crack ratio decreases rapidly.

2) The amount of cracks on the nonloading surfaces is bigger than that of the loading surfaces. Diagonal cracks formed on the nonloading surfaces. Horizontal cracks formed on the loading surfaces.

3) In case of higher axial load, the amount of cracks is less, and the amount of spalling is bigger than that of lower.

REFERENCES

1. Shibata, A., and Sozen, M. A., "Substitute-Structure Method for Seismic Design in R/C", Journal of St. Div., ASCE, Vol. 102, No. ST1, (1976).
2 Banon, H., Biggs, J. M., and Max Irvine, H., "Seismic Damage in Reinforced Concrete Frames", Journal of St. Div., ASCE, Vol. 107, No. ST9, (1981).
3 Toussi, S., Yao, J. Y. P., and Chen, W. F., "A Damage Indicator for Reinforced Concrete Frames", ACI Journal, Vol. 81, No. 3, (1984).
4. Darwin, D, and Nmai, C. K., "Energy Dissipation in RC Beams under Cyclic Load", Journal of St. Div., ASCE, Vol. 112, No. 8, (1986).
5. List of Experimental Results on dynamic Properties of Reinforced Concrete Columns Under Inelastic Load Reversals (in Japanese), Building Research Institute, Ministry of Construction, Japan, 1975-1977.
6. Priestley, M. J. N., and Park, R., "Strength and Ductility of Concrete Bridge Columns Under Seismic Loading," ACI Structural Journal, Vol. 84, No. 1, (1987).
7. Low, S. S. and Moehle, J. P., "Experimental Study of Reinforced Concrete Columns Subjected to Multi-axial Cyclic Loading," Earthquake Research Center Report UBC/EERC-84/14, University California, Berkeley, (1987).

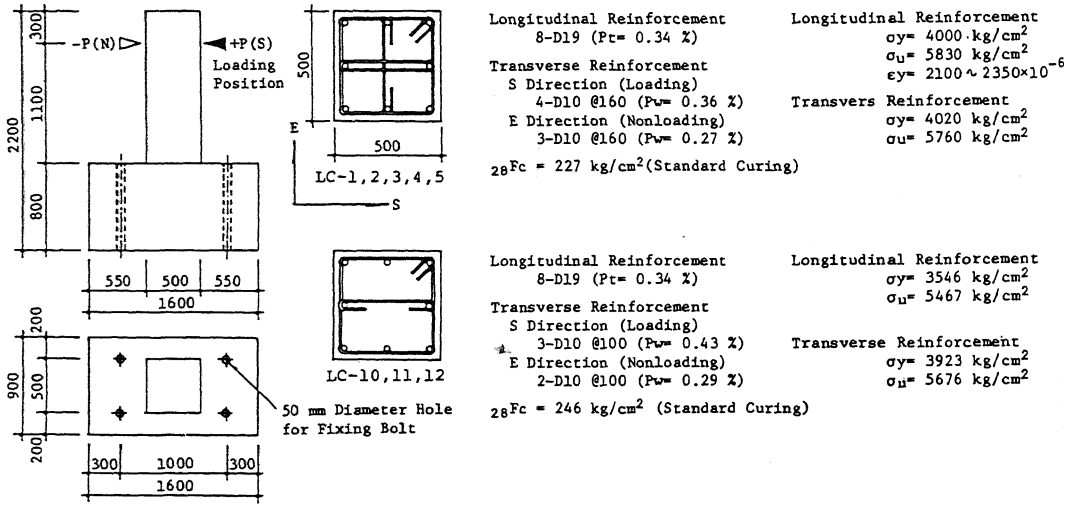

Fig. 1 Test Specimen Configuration and Reinforcement

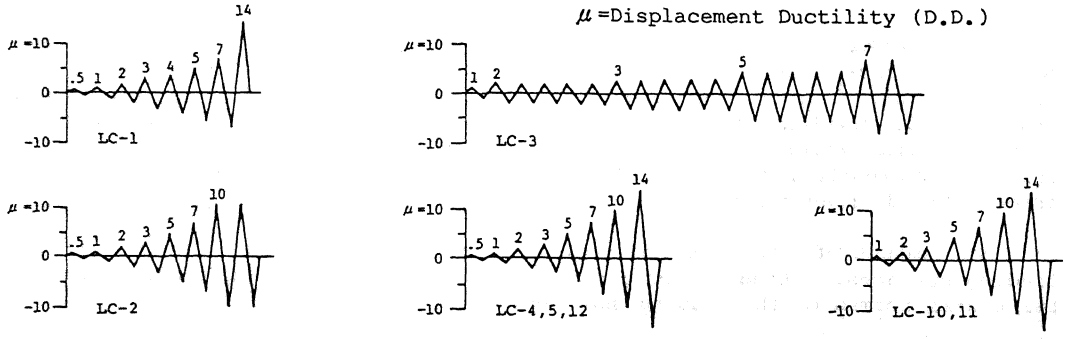

Fig. 2 Intended Displacement Load Histories for Each Test Specimen

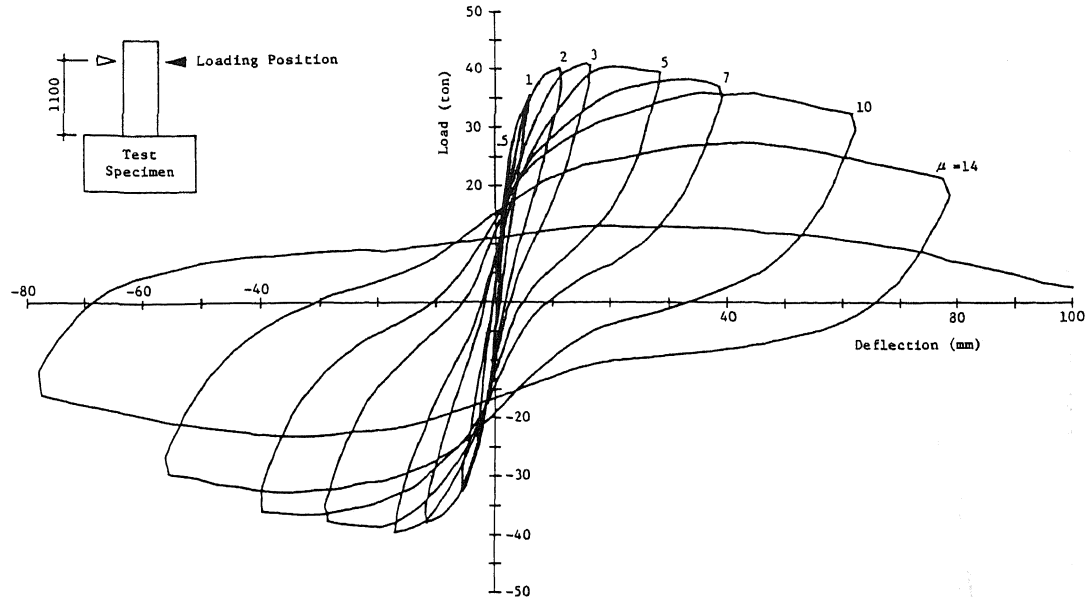

Fig. 3 Load-Displacement Hysteresis Loops of Specimen LC-12

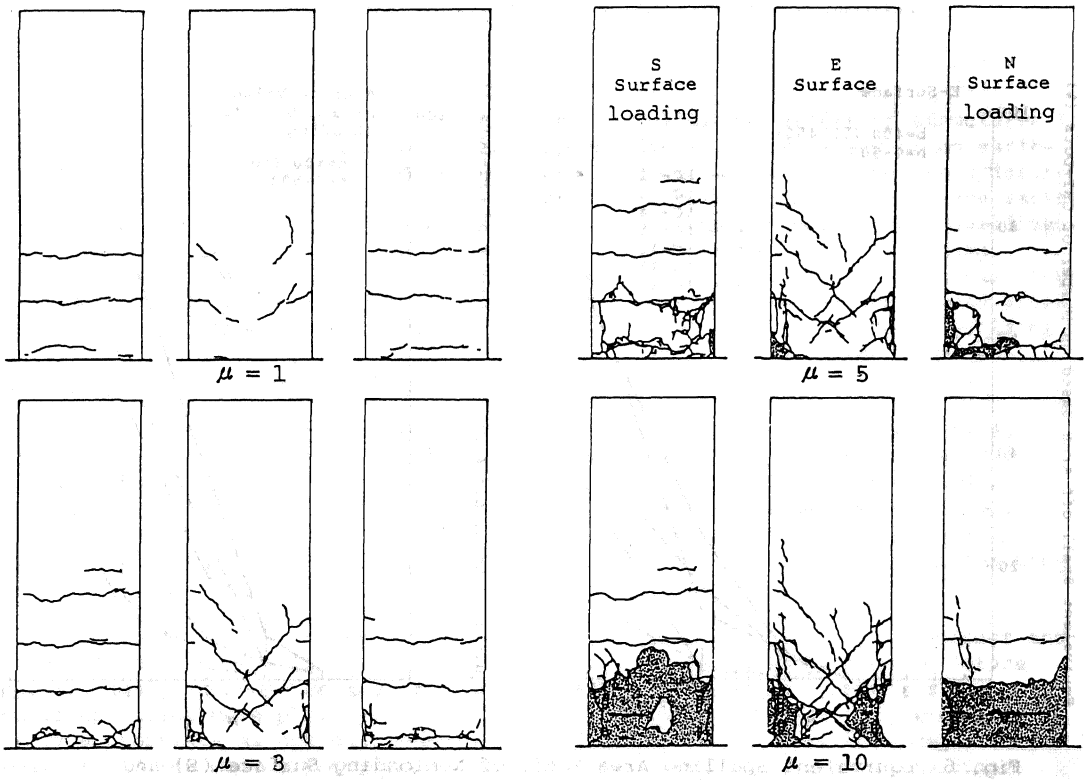

Fig. 4 Crack and Spalling Diagrams of Specimen LC-12

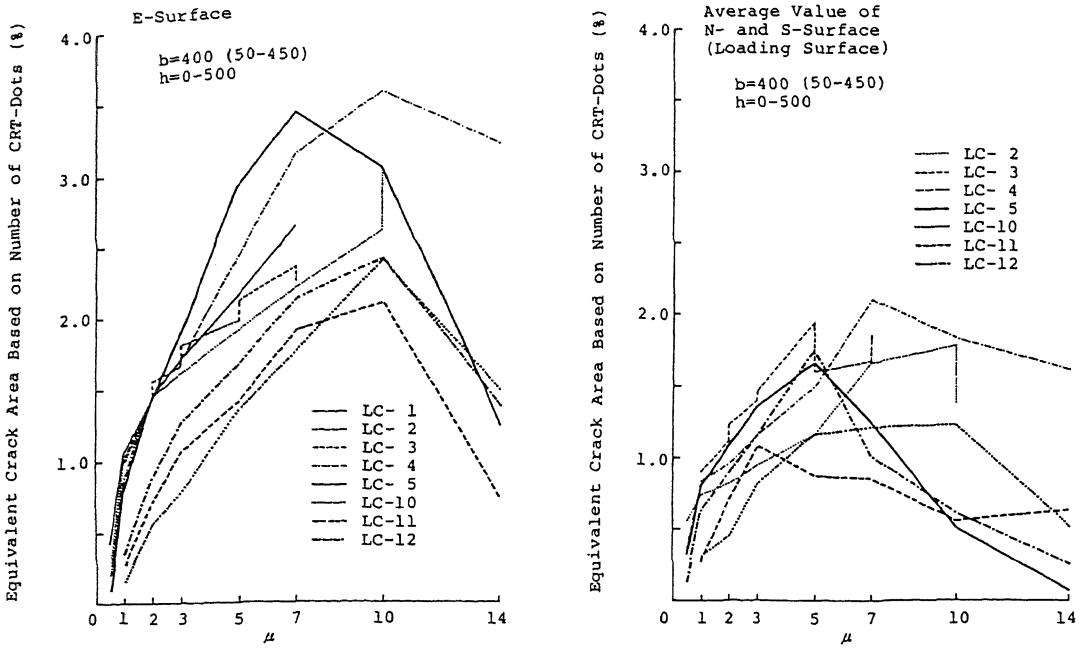

Fig. 5 Equivalent Crack Area Ratio of Nonloading Surface (E) and Loading Surface (N and S) at Different Displacement Ductilities

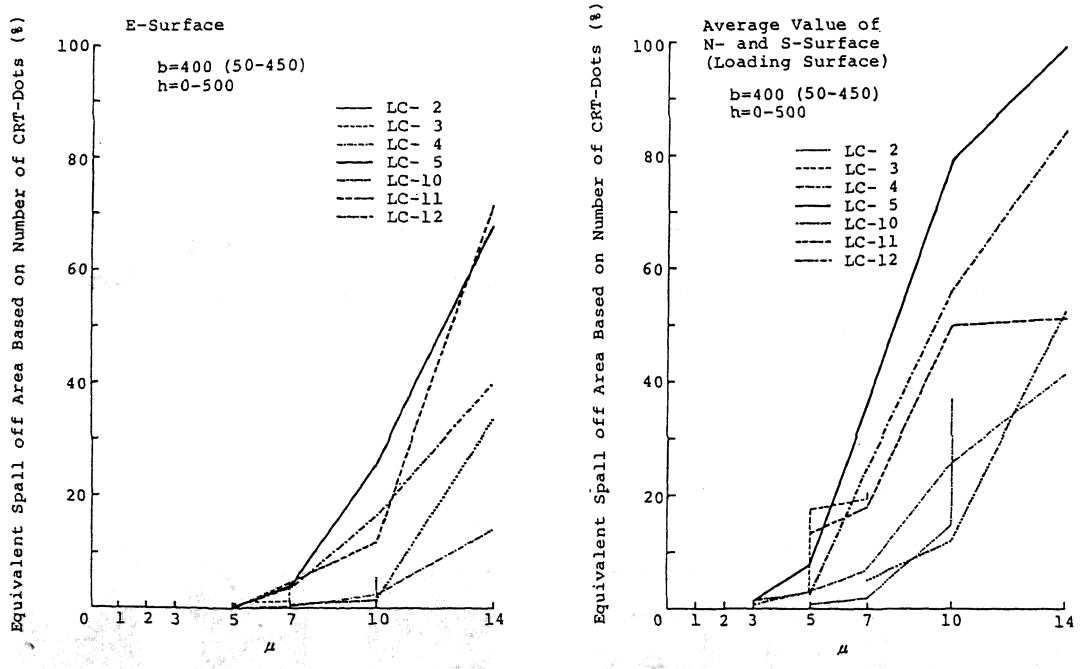

Fig. 6 Equivalent Spalling Area Ratio of Nonloading Surface (E) and Loading Surface (N and S) at Different Displacement Ductilities